Available online at www.sciencedirect.com
SCIENCE DIRECT
Journal of Catalysis 241 (2006) 189–199
JOURNAL OF CATALYSIS
www.elsevier.com/locate/jcat

Chemical and kinetic study of acetophenone hydrogenation over Pt/Al_2O_3: Application of BTEM and other multivariate techniques to quantitative on-line FTIR measurements

Feng Gao [a], Ayman D. Allian [a], Huajun Zhang [b], Shuying Cheng [a], Marc Garland [a,b,*]

[a] *Department of Chemical and Biomolecular Engineering, 4 Engineering Drive 4, National University of Singapore, Singapore 117576*
[b] *Institute of Chemical and Engineering Science 1, Pesek Road, Jurong Island, Singapore 627833*

Received 25 February 2006; revised 23 April 2006; accepted 24 April 2006

Abstract

The heterogeneous catalytic hydrogenation of acetophenone (Aceph) over Pt/Al_2O_3 in d_8-toluene/h_8-toluene at 273 K was performed in semibatch mode, using a recycle configuration and on-line quantitative Fourier transform infrared (FTIR) spectroscopy measurements. Based on the d_8-toluene solvent used and the multivariate analysis applied, further details of the reaction chemistry were elucidated, including the following: (i) Solvent activation occurred during reaction, leading to observable hydrogenation and H–D exchange, and (ii) 1-phenylethanol (Phel), cyclohexyl methyl ketone (CMK), and cyclohexylethanol (Che) were observable products, and little H–D exchange occurred. The on-line FTIR measurements, with sensitivity on the order of 10^{-5} mol/L, also lead to the following kinetic observations: (i) Water had a strong inhibiting effect on the hydrogenation rates, and (ii) very interesting short time-scale kinetic behavior occurred after some perturbations. The latter included rapid initial hydrogenations on fresh catalyst (due to the presence of spillover hydrogen) and observable adsorption–desorption of other reactants. The reaction rates obtained from the well-defined experiments in h_8-toluene were fit to a number of Langmuir–Hinshelwood–Hougen–Watson (LHHW) models, in which the effects of solvent and water were included. A model involving a pairwise addition of adsorbed dissociated hydrogen to the adsorbed substrate provided the best fit of the data. The regression of the kinetic data suggested that water made a statistically significant contribution to the competitive adsorption on the catalyst surface. In more general terms, the present contribution suggests the utility of detailed on-line liquid-phase spectroscopy together with multivariate techniques for exploratory studies of heterogeneous catalytic systems.

Keywords: Heterogeneous catalysis; Recycle reactor; On-line FTIR spectroscopy; Multiple perturbations; BTEM/tBTEM; LHHW model

1. Introduction

The catalytic hydrogenation of carbonyl groups is an important class of reactions in the fine-chemical and pharmaceutical industries [1]. The hydrogenation of acetophenone is of particular interest because of the primary reaction product 1-phenylethanol (Phel), which is used extensively in the pharmaceutical and perfume industries [2]. Earlier studies concerning heterogeneous catalytic hydrogenation of acetophenone were performed on Pd, Pt, Ni, and Ru catalysts at various temperatures and pressures [3–16]. Under many reaction conditions, in addition to the primary product, Phel, two common side products are cyclohexyl methyl ketone (CMK) and cyclohexyl ethanol (Che). The product distribution has been shown to be strongly dependent on reaction conditions and catalyst composition. Platinum is a good catalyst for hydrogenation of both carbonyl and phenyl groups. Acetophenone hydrogenation on Pt catalysts produces marked amounts of CMK and Che as co-products [9,10,12,16]. At elevated temperatures, ethyl cyclohexane, ethyl benzene, styrene, toluene, and benzene have also been reported as possible side products. An overview of the primary product distribution in the liquid-phase syntheses at low temperatures is provided in Fig. 1.

A versatile and compact experimental apparatus, consisting of a stirred tank (25 mL), pump, tubular reactor, on-line

* Corresponding author.
E-mail address: chemvg@nus.edu.sg (M. Garland).

0021-9517/$ – see front matter
doi:10.1016/j.jcat.2006.04.024

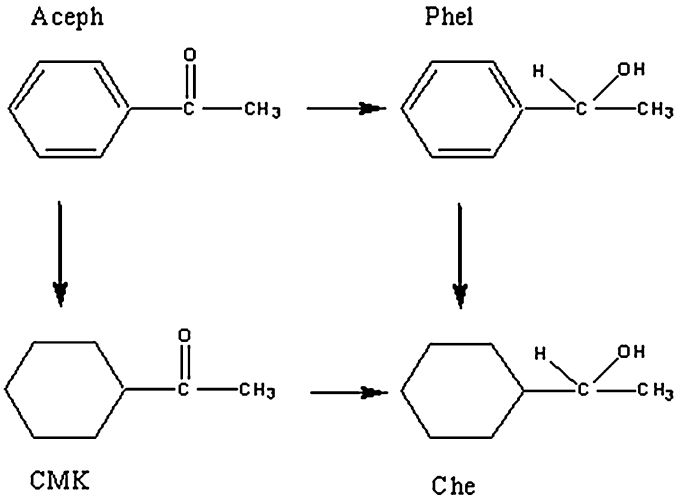

Fig. 1. The possible reactions in the liquid-phase heterogeneous hydrogenation of Aceph over Pt/Al_2O_3 at low temperatures and low hydrogen pressures.

Fourier transform infrared (FTIR) spectrometer, and an injection/sampling block for liquid-phase perturbations, was designed and characterized with respect to gas–liquid mass transfer, mixing, liquid–solid mass transfer, and intraparticle diffusion [17]. This setup was used in the current study to address chemical issues associated with using d_8-toluene as a solvent, as well the kinetic issues associated with using h_8-toluene as a solvent. The present setup and methodology provided several advantages for liquid-phase analyses. First, due to the on-line FTIR measurements, concentrations of solutes could be measured quickly and with high precision, and the instantaneous reaction rates could be evaluated very accurately. These aspects greatly facilitated the least squares regression of LHHW models as well as comparisons among models, because more data were available and the quality of this data was higher. Second, multiple reagent perturbations allowed coverage of a wide range of experimental conditions in a single semibatch run. These multiple perturbations also greatly facilitated the application of two advanced signal-processing programs, band-target entropy minimization (BTEM) [18–22] and two-band-target entropy minimization (tBTEM) [23], thus permitting high-quality deconvolution of the pure component spectra present. The benefits of on-line multivariate analysis for calibration and system identification, in contrast to off-line univariate measurements, are widely recognized [24].

With a total liquid-phase volume of only ca. 15 mL, the experimental apparatus permitted the use of an isotopically labeled solvent. By using a special solvent for spectroscopic purposes, very specific chemical issues could then be addressed by the on-line FTIR measurements and multivariate analysis. d_8-toluene was chosen as a solvent because it is readily available in high purity. This solvent allowed use of the C–H infrared spectral region near 3000 cm^{-1} for quantitative analysis of all of the species involved in catalytic hydrogenation. Using d_8-toluene also allowed observation of the competitive hydrogenation of the solvent. A further advantage of toluene over more common solvents, like ethanol for this reaction, is the ease of distillation to a very anhydrous state, thereby allowing better understanding of the role of water in the catalysis.

The detailed kinetic analysis of acetophenone (Aceph) hydrogenation over Pt/Al_2O_3 to 1-phenylethanol (Phel) in h_8-toluene was also performed. Again, quantitative information was obtained by on-line FTIR measurements together with multivariate analysis. Based on the concentration profiles and rates thus obtained, various LHHW models were fit, and conclusions were drawn concerning the most appropriate model.

The principle aim of the present contribution was to demonstrate that the judicious choice of experimental configuration and numerical techniques can provide new and further opportunities and insights into this well-studied reaction. Moreover, the general methodological issues raised are in fact applicable to many other fine-chemical liquid-phase heterogeneous catalytic reactions.

2. Experimental

2.1. General issues

2.1.1. Chemicals

The catalyst Engelhard 4759 (5% Pt/Al_2O_3) was sieved, and the fraction from 53 to 75 μm was used in this study. It was prereduced in H_2 at 400 °C for 120 min before reaction [25]. This catalyst was characterized elsewhere [26]. d_8-toluene (99.6%, Cambridge Isotope Laboratories) and toluene (99.9%, Mallinckrodt) were distilled from sodium–potassium alloy under purified argon for ca. 5 h to remove the trace water and oxygen. Acetophenone (99%, Aldrich) and 1-phenylethanol (98%, Acros Organics) were mixed and shaken with anhydrous 4-Å molecular sieves to remove traces of water. Deionized water was used without further purification. The other chemical standards used included CMK (Aldrich) and Che (98%, Avocado).

2.1.2. Experimental apparatus and on-line analytics

The experimental system consisted of a stirred tank (25 mL), pump, tubular reactor, on-line FTIR spectrometer, and injection/sampling block for liquid-phase perturbations, all in a closed-recycle configuration. Standard Schlenk techniques [27] were used in all of the experiments. The general experimental procedures and details of the apparatus have been described elsewhere [17]. The pressure of hydrogen was kept almost constant during each experiment using a 1-L reservoir connected to the system. The liquid was kept saturated with hydrogen by operating the stirred tank at a stirring speed of 400 rpm. The packed-bed tubular reactor with ca. 0.02 g of catalyst was immersed in a water bath (Polyscience 9505) at 0 °C. A heat exchanger, consisting of ca. 60 cm of SS316 1/16-inch tubing, was positioned before the reactor in the water bath. The remaining parts of the experimental apparatus were maintained at room temperature (ca. 22 °C).

The FTIR spectrometer was a Perkin–Elmer spectrum 2000 with a deuterated triglycine sulfate detector. The spectral resolution was 4 cm^{-1} with a data interval of 0.2 cm^{-1} for the range 1000–5000 cm^{-1}. Purified nitrogen (99.99%, Saxol) was

used to purge the FTIR spectrometer system. The path length of the sturdy high-pressure FTIR cell with 15-mm-thick CaF_2 windows was constant at ca. 0.0371 cm. The pressure dependence of the cell's path length, in the interval of 1.0–3.0 bar, can be neglected in this study.

2.1.3. Off-line analytics

A gas chromatograph–mass spectrometer (GC, Hewlett–Packard 6890; MS, Hewlett–Packard 5973) with a HP-5MS column (30 m × 0.25 mm × 0.25 μm) or a ZB-5 column (30 m × 0.25 mm × 0.25 μm) was used in this study.

2.1.4. Band-target entropy minimization

Both BTEM and tBTEM were used to obtain pure component spectral estimates from the multicomponent liquid phase [18–23]. Often, the BTEM/tBTEM estimates were more accurate than authentic references, because spurious moisture signals, etc., were eliminated. In the final fitting of the pure component spectra to the measured reaction spectra, almost 100% of the experiment signal could be recovered. Further details regarding the application of BTEM/tBTEM to acetophenone hydrogenation in d_8-toluene and h_8-toluene are provided in the supplementary material (Parts 1 and 2).

2.1.5. Mass balances and molar absorptivities

The Lambert–Beer law was used to obtain the species concentrations from the reactive FTIR absorbance spectra. Details on using the Lambert–Beer expression for quantitative in situ or on-line measurements of liquid phases and the determination of concentrations, overall mass balances, and rates have been given previously [17,28].

The molar absorptivities of the different species were obtained from dilute solutions with different concentrations using d_8-toluene or h_8-toluene as the solvent. Calibrations were performed, and the molar absorptivities of Aceph (at ca. 3064 and 1690 cm^{-1}), Phel (at ca. 3579 cm^{-1}), Che (at ca. 2931 cm^{-1}), and water (at ca. 3680 cm^{-1}) were determined to be ca. 22.2, 619.1, 73.2, 393.6 and 73.7 L/(mol cm), respectively. Based on some judicious comparisons with the related compounds, approximate values of 400, 150, and 410 L/(mol cm) were chosen for the absorptivities of d_8–h_6 methylcyclohexane at ca. 2903 cm^{-1} and CMK at ca. 1710 and 2931 cm^{-1}. d_8–h_6 methylcyclohexane was the primary product for the hydrogenation of d_8-toluene over Pt/Al_2O_3.

Multivariate analysis of the d_8-toluene experiment was performed over the entire spectral window of 2500–4000 cm^{-1}. Due to the strong C–H vibrations, multivariate analyses of the h_8-toluene kinetic experiments were performed over two spectral windows of 1650–1750 and 3200–4000 cm^{-1}. Further details of the multivariate analysis are provided in the supplementary material (Parts 1 and 2). Multivariate analysis of the experimental spectra on the intervals at 2500–4000 cm^{-1} and 3200–4000 cm^{-1} included the use of background/moisture spectra to obtain proper modeling for the O–H vibrational region.

2.1.6. Mass transfer issues

As demonstrated in detail elsewhere [17], the kinetic studies performed in h_8-toluene were not (i) gas–liquid mass transfer-controlled at 400 rpm; (ii) liquid–solid mass transfer-controlled at a flow rate of 5 mL/min, or (iii) intraparticle diffusion-controlled using 53–75 μm catalyst particles. In the experiment performed in d_8-toluene, a flow rate of ca. 3 mL/min was used. This suboptimal flow rate decreased the observable rate slightly (on the order of $\leqslant$20%).

2.1.7. The maximum observable reaction rates

Under current reaction conditions, the maximum observable rates of hydrogenation were ca. 6×10^{-5} mol/(min g_{cat}) (Aceph to Phel), ca. 1×10^{-5} mol/(min g_{cat}) (Aceph to CMK), and ca. 2×10^{-6} mol/(min g_{cat}) (Phel to Che). The hydrogenation of Aceph to Phel was the predominant reaction present. In this study, the conversion for Aceph per pass was <0.5%. Accordingly, the present reaction was carried out under differential conversion in each pass. This is often an important consideration for accurate kinetic modeling [29]. The reaction rates were calculated based on the slopes of the concentration profiles of Phel, CMK, and Che, and these were evaluated on 10-spectra intervals.

2.2. Experimental design

To study the chemical issues involved in the acetophenone hydrogenation, one semibatch reaction with perturbations of substrate acetophenone (Aceph), product 1-phenylethanol (Phel), and water were performed in d_8-toluene at 0 °C and 1.56 bar hydrogen partial pressure. The details of the perturbations are given in Table 1. The solution was pumped throughout the experimental system at a rate of ca. 3 mL/min.

A total of six well-defined experiments with multiple perturbations were conducted in h_8-toluene to study the reaction kinetics of Aceph hydrogenation to Phel at 0 °C. Four different hydrogen partial pressures, five 20-μL Aceph perturbations, and

Table 1
Experimental design for the semibatch in d_8-toluene reaction, using Pt/Al_2O_3 catalyst and on-line FTIR measurements. Perturbations were performed at various reaction times using injections of Aceph, Phel or water through the rotary HPLC valves mounted in the on-line injection/sampling block

Time (min)	Spectral no.	Volume of substrate injected (μL)	Volume of Phel injected (μL)	Volume of water injected (μL)
10	10	20		
40	36	20		
70	63	20		
100	91	20		
130	114	20		
175	154		2	
205	180		2	
235	206		2	
265	232			2
295	258			2
319	279			2
345 = end	300			

Table 2
The experimental designs for the kinetic study of acetophenone hydrogenation to 1-phenylethanol over Pt/Al_2O_3 in h_8-toluene

Expt. no.	Catalyst load (g)	Steps	P_{H_2} (bar)	Substrate (μL)	Product (μL)
1	0.020	1	1.75	20	
		2	1.75	20	
		3	1.75	20	
2	0.019	1	1.75	60	
		2	1.75	20	
		3	1.75	20	
3	0.019	1	1.75	60	
		2	1.75		2
		3	1.75		2
		4	1.75		2
		5	1.75		2
4	0.020	1	2.49	60	
5	0.019	1	2.98	60	
6	0.019	1	1.28	60	

four 2-μL Phel perturbations were included. The detailed experimental designs of the six experiments are given in Table 2.

3. Results

3.1. The chemistry in d_8-toluene as solvent

3.1.1. Concentration profiles

The concentration profiles of the organic reagents during the reaction are plotted in Fig. 2, and the concentration profiles of the remaining species d_8-toluene, water, and d_8–h_6 methylcyclohexane are plotted in Fig. 3. The concentrations of d_8-toluene during reaction were obtained by comparing them to the pure reference (9.36 M). It is important to note that the sensitivity of the on-line FTIR measurements, as indicated by the sequential data points in Fig. 2d, is ca. 10^{-5} mol/L. Typical concentration perturbations were on the order of 10^{-3}–10^{-2} mol/L, which can be readily identified in the plots.

Throughout the study, good mass balances were obtained, even after multiple perturbations were performed. For example, during the period from spectrum 140 to spectrum 300 (i.e., after the fifth perturbation of Aceph; see experimental design Table 1), the decrease in Aceph was ca. 1.4×10^{-4} mol. Also during this period, a total of 1.3×10^{-4} mol of Phel were injected. This is consistent with the total increases of Phel, CMK, and Che, which were ca. 2.7×10^{-4} mol. It is important to mention that due to the use of the rotary valves, 3×2 μL of system solution was lost in the same period. However, the loss of 6 μL from the ca. 15,000-μL solution can be considered negligible for the present discussion.

3.1.2. Perturbations and on-line measurements

The experimental design, according to Table 1, involved a series of perturbations in the substrate Aceph, the primary product Phel, and water. These perturbations were planned to survey a wide range of reactions conditions rapidly and with a minimum usage of resources, and obtain spectroscopic data particularly suitable for deconvolution via the BTEM/tBTEM algorithm.

3.1.2.1. Substrate perturbations The first set of perturbations involved injections of substrate. In Fig. 2a, the concentrations of the substrate as a function of spectral number are shown.

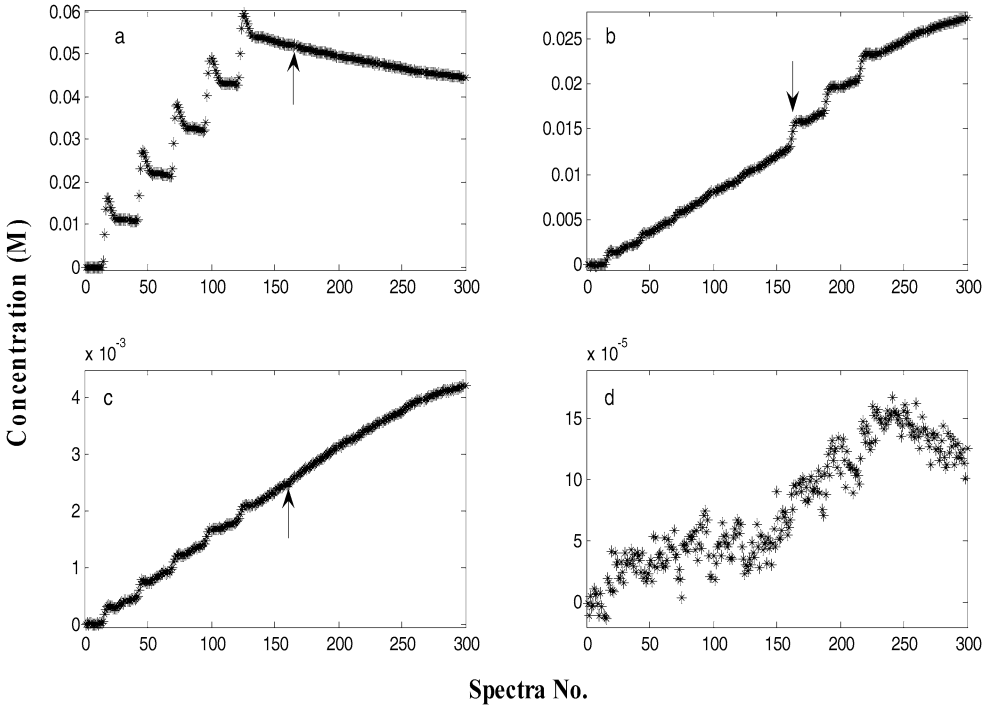

Fig. 2. The concentration profiles of the organic reagents during the piece-wise continuous reaction in d_8-toluene involving numerous perturbations. (a) Aceph; (b) Phel; (c) CMK; (d) Che. The three arrows in (a), (b), and (c), corresponding to the 165th spectrum, indicate the first perturbation of Phel.

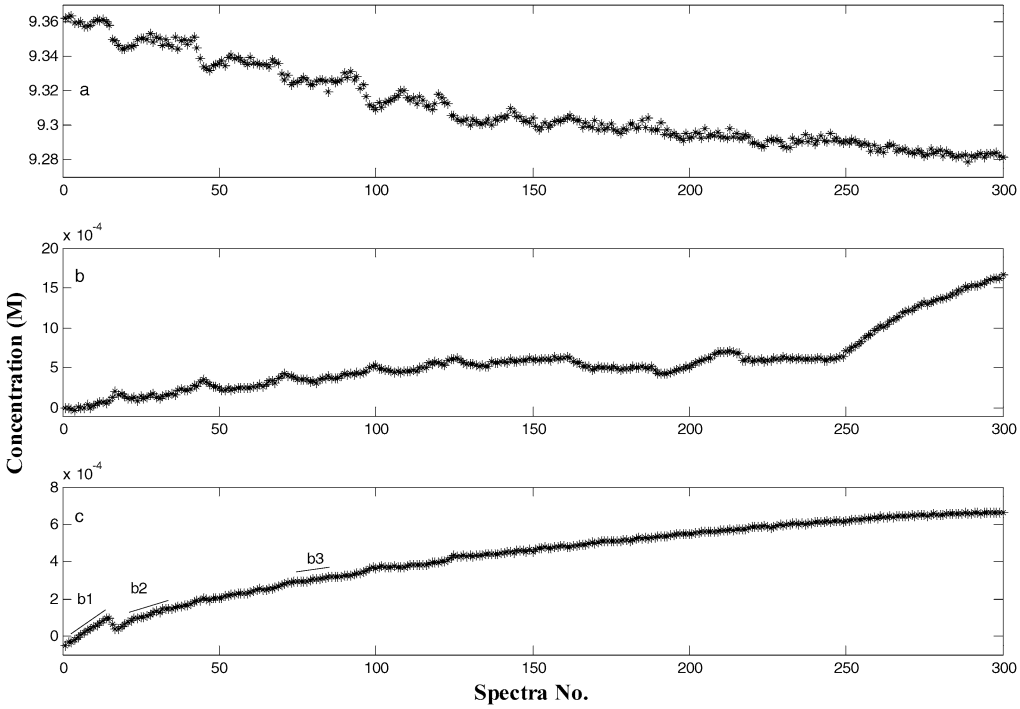

Fig. 3. The concentration profiles of d_8-toluene, water and d_8–h_6 methylcyclohexane during the reaction. (a) d_8-toluene; (b) water; (c) d_8–h_6 methylcyclohexane. The slopes b1–b3 indicate the rates of the formation of d_8–h_6 methylcyclohexane during the data points 1–15, 20–35 and 74–84, respectively.

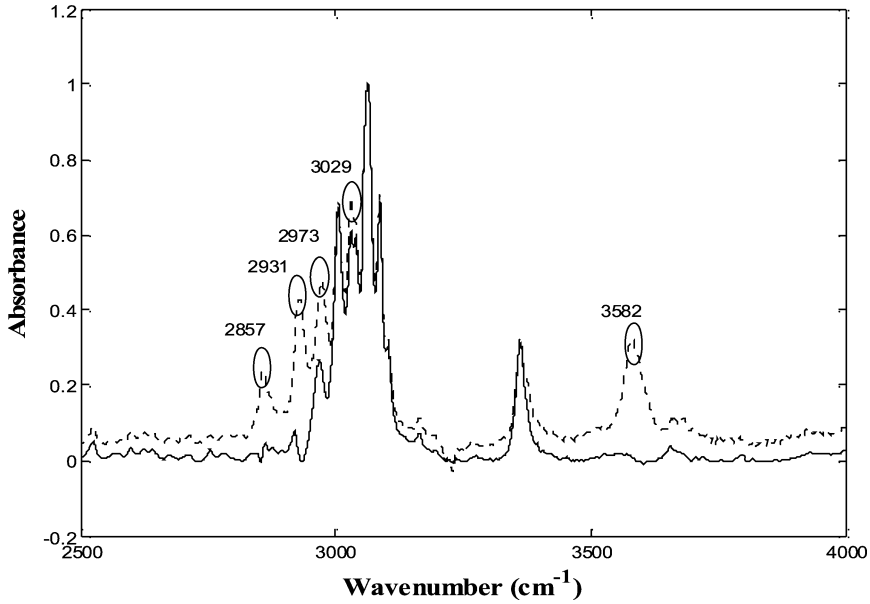

Fig. 4. Comparison of the normalized spectral changes (- - -) occurring after 1st perturbation of substrate with normalized reference spectrum of substrate (—).

The five perturbations of the substrate are readily identified in the first 155 data points. The overshoot immediately after an injection is due to the well-known dynamics of a closed recycle reaction configuration [30]. Indeed, a separate experiment with this apparatus involving injections of d_8-toluene into h_8-toluene in the absence of catalyst produced the same type of dynamics [17]. In Figs. 2b and 2c, and during the first 155 data points, very interesting and unexpected rapid increases in the concentrations of the products Phel and CMK were observed immediately after each substrate perturbation. The magnitude of the increases in concentration after each perturbation appeared to decline as a function of the number of perturbations performed.

The observation of unusually rapid increases in the concentrations of the products Phel and CMK (compared with their long-term rates) is certainly real and not an artifact of the multivariate analysis. This can be clearly demonstrated by comparing spectra immediately before and after an injection. As an illustration, Fig. 4 shows the normalized 18th experimental spectrum (with solvent subtraction) taken after the first substrate perturbation is compared with a normalized spectrum

of substrate. The strong, highlighted new bands belong to the products.

3.1.2.2. Phel perturbations The second set of perturbations involved injections of the primary product Phel. Fig. 2b shows the concentrations of Phel as a function of spectral number are shown. The three perturbations of Phel are readily identified during the 156–230th data points. Phel overshoots, associated with the recycle configuration, were observed in these perturbations.

3.1.2.3. Water perturbations The third set of perturbations involved injections of water. Three perturbations of 2 μL of water were performed at the 232th, 258th, and 279th experimental spectra. Sharp jumps in the dissolved water concentration were not observed due to the slow dissolution kinetics. However, clear decreases in the slopes of Phel and CMK were apparent starting at the 250th spectrum. The concentrations of Che appear to actually decrease, but due to the very low signal intensities involved, this is most likely an artifact of the multivariate fitting. The formation rates of Phel and CMK were ca. 4.7×10^{-5} mol/(min g_{cat}) and ca. 7.6×10^{-6} mol/(min g_{cat}) at the 250th spectrum and ca. 2.5×10^{-5} mol/(min g_{cat}) and ca. 4.7×10^{-6} mol/(min g_{cat}) at the 300th spectrum. There was a clear decrease in the reaction rates.

To summarize, the perturbation experiments described in Section 3.1.2 indicate that the catalytic system responded on two different time scales. The first scale was a brief system response, reactive as well as nonreactive, to the perturbations. The second was a longer time scale response due to the reaction kinetics alone.

3.1.3. Chemical issues

Several samples including the reaction mixture were also analyzed using a GC-MS to provide further information on (i) hydrogenation of the d_8-toluene, (ii) possible d_8-toluene H–D exchange with other reactants, and (iii) the product distribution, as exemplified by Fig. 1. Further details on GC-MS analysis are given in the supplementary material (Part 3).

3.1.3.1. Solvent chemistry A separate catalytic Schlenk tube experiment with only d_8-toluene, H_2, and Pt/Al_2O_3 was performed. Clear FTIR and GC-MS experimental evidence (i.e., strong broad vibration at 2903 cm^{-1} and significant fragment at 106 m/z, were obtained for hydrogenation of d_8-toluene to d_8–h_6 methylcyclohexane. In addition, other fragments at 92, 93, 95, and 96 m/z provided evidence for H–D exchange on the d_8-toluene, and fragments at 104, 105, 107, and 108 m/z provided evidence of H–D exchange on the hydrogenated product. The FTIR and GC-MS results were then used to confirm the presence of both phenomena in the acetophenone hydrogenation experiment.

In the acetophenone hydrogenation experiment in d_8-toluene, only slight hydrogenation of the solvent occurred (ca. 0.01%). The slopes b1–b3 in Fig. 3c indicate the rates of formation of d_8–h_6 methylcyclohexane during the data points 1–15 (before the first Aceph perturbation), 20–35 (after the first Aceph perturbation), and 74–84 (after the third Aceph perturbation), respectively. In the first period, only solvent was present, and a high rate of formation of d_8–h_6 methylcyclohexane occurred. Afterward, the rates of formation of d_8–h_6 methylcyclohexane clearly decreased with increasing Aceph. These reduced rates of solvent hydrogenation can be rationalized by noting that acetophenone should have a much higher adsorption equilibrium constant than toluene and thus can successfully displace d_8-toluene on the platinum surface. With less adsorbed toluene, little hydrogenation and H–D exchange of d_8-toluene can occur.

3.1.3.2. Reactants The on-line FTIR measurements and multivariate analysis (BTEM/tBTEM) of the acetophenone hydrogenation experiment over Pt/Al_2O_3 in d_8-toluene revealed only d_8-toluene, d_8–h_6 methylcyclohexane, Aceph, Phel, CMK, Che, and water as observable liquid-phase components. GC-MS analysis of the reaction mixture confirmed the presence of Aceph, Phel, CMK, and Che (as well as their isotopomers, with ca. 1% H–D exchange), but no other organic reactants. In particular, there was no evidence of ethylcyclohexane, ethylbenzene, styrene, toluene, or benzene. Accordingly, Fig. 1 accurately represents the product distribution for the liquid-phase acetophenone hydrogenation under the reaction conditions used.

3.2. Kinetic study performed in h_8-toluene

Using d_8-toluene as the solvent in the preliminary experiment helped clarify the chemical issues. To address the associated kinetic issues, the solvent was changed from d_8-toluene to h_8-toluene. Two spectral regions, at 1650–1750 and 3200–4000 cm^{-1}, were selected for the multivariate quantitative spectral analysis in the kinetic study using h_8-toluene as the solvent. The first region corresponds to the carbonyl fundamental vibrational; the second, to the O–H fundamental vibrational and carbonyl overtone. In the second spectral window, CMK had a very weak carbonyl overtone, and Che had a hydroxyl absorptivity of ca. 70 L/(mol cm). Furthermore, in the present study, the selectivity to CMK was <20% and the selectivity to Che was <3%. But, most importantly, the maximum conversion of Aceph was only ca. 25%. Accordingly, both CMK and Che made very small contributions to the overall experimental absorbance in the second spectral region. After trying various fitting procedures to account for the very small contributions involved, these two species were neglected from the multivariate quantitative spectral analysis. Quantitative information on the instantaneous concentrations of Aceph, Phel, and water were obtained by multivariate analysis of the two spectral windows mentioned.

As seen in the d_8-toluene experiment, the on-line FTIR measurements in h_8-toluene indicated two different time scales for observable events. In this section, attention is given to this complex superposition of effects, whereas in Section 3.3, only modeling and analysis of the long time scale reaction kinetics is addressed.

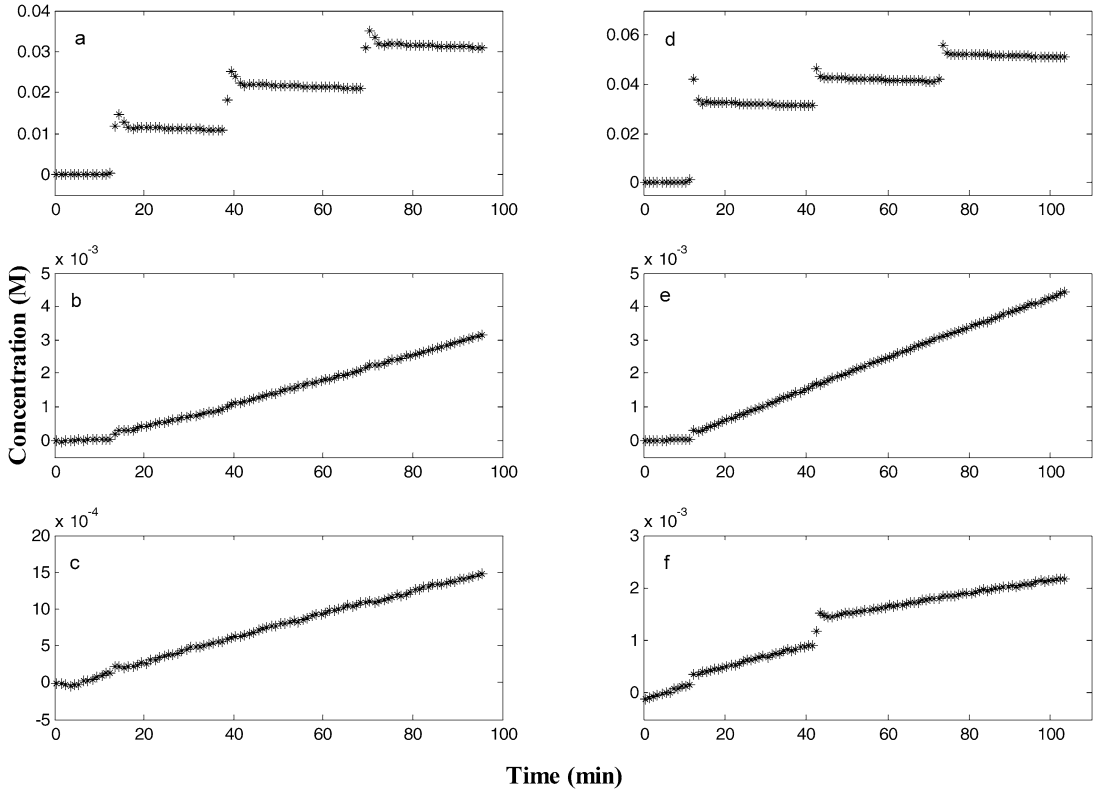

Fig. 5. The concentration profiles of different species in Expt. 1 and Expt. 2. (a) Aceph in Expt. 1; (b) Phel in Expt. 1; (c) water in Expt. 1; (d) Aceph in Expt. 2; (e) Phel in Expt. 2; (f) water in Expt. 2.

3.2.1. *Different substrate concentrations and the reaction rates*

Experiments 1 and 2 were performed to address the effect of different substrate concentrations on the reaction rates. In experiment 1, three injections of 20-μL acetophenone were introduced using the injection valves in one semibatch experiment. In experiment 2, 60 μL of acetophenone was first injected into the reaction system at time $t = 10$ min. Afterward, two perturbations of the substrate acetophenone in 20-μL volumes were injected. Concentration profiles of the substrate, product Phel, and water in experiments 1 and 2 are plotted in Fig. 5.

Fig. 5 shows smooth piecewise continuous concentration profiles for all of the solutes. As expected, each perturbation of substrate Aceph resulted in a momentary overshoot in the Aceph concentration profile due to the closed-recycle configuration, followed by gradually decreasing concentration due to reaction. The Phel concentration took an initial jump, followed by gradual concentration increases due to the reaction. The dissolved water concentration (i) continuously increased due to slow desorption from the experimental system and subsequent dissolution into the anhydrous liquid phase and (ii) discontinuously increased due to introduction during perturbations. A representative example of case (ii) is the obvious jump in the water concentration after the second perturbation of Aceph, occurring at the 44th data point in Fig. 5. In this regard, it is important to recognize the presence of residual moisture in the treated reagents, as well as the logistic difficulties associated with performing entirely anhydrous transfers.

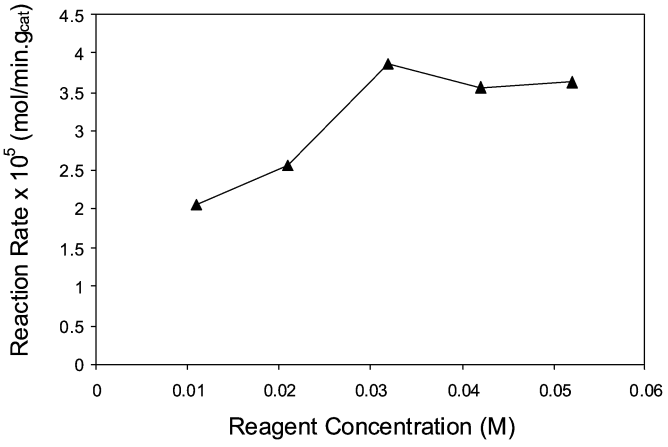

Fig. 6. The reaction rates for the formation of 1-phenylethanol as a function of different substrate concentrations.

The formation rates of 1-phenylethanol at the different substrate concentrations are plotted in Fig. 6. This figure shows that at low concentrations of acetophenone, the formation rate of Phel increased with increasing concentration of acetophenone, whereas at high concentrations and higher conversions, the rates were almost independent of acetophenone concentration.

3.2.2. *Different Phel concentrations and the reaction rates*

Experiment 3 was performed to address the effects of different product concentrations on the reaction rates. First, 60 μL of acetophenone was injected into the reaction system at time

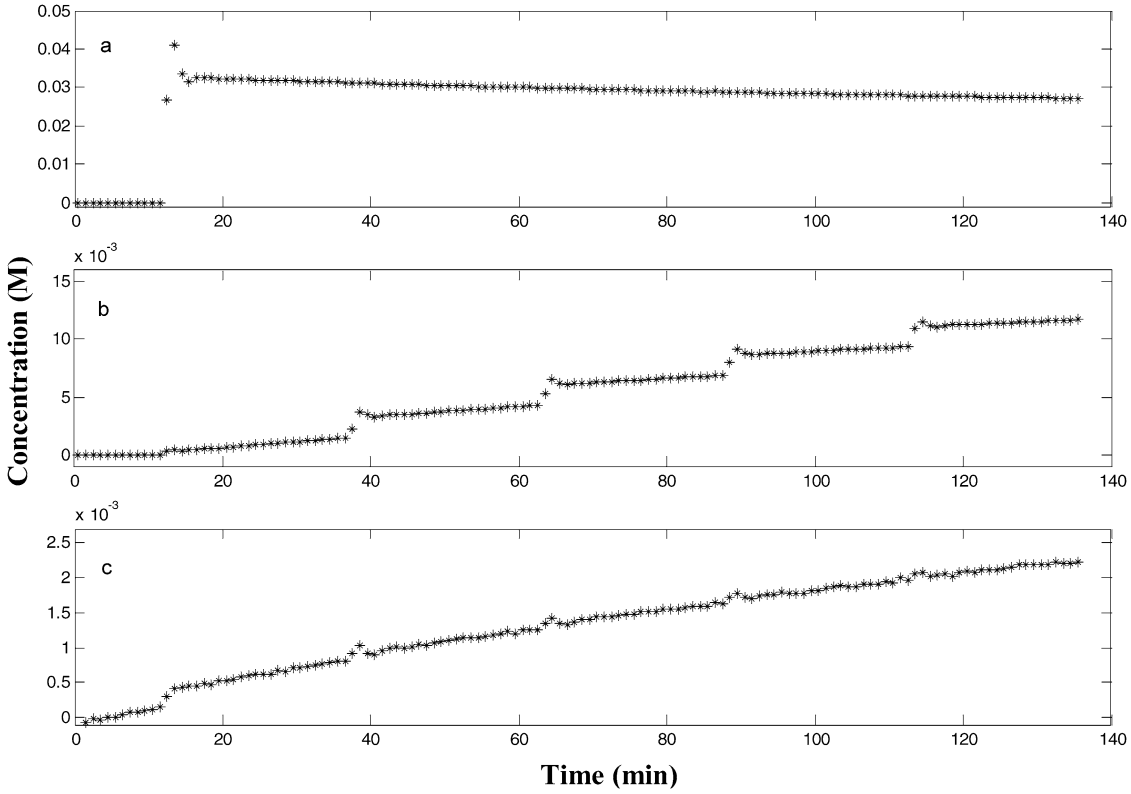

Fig. 7. The concentration profiles of Aceph, Phel and water with 4 different Phel perturbations performed at times 36, 62, 87 and 112 min. (a) Aceph; (b) Phel; (c) water.

$t = 10$ min; then four perturbations of 1-phenylethanol (2 μL each) were sequentially injected into the reaction system. Concentration profiles of the substrate, product Phel, and water are plotted in Fig. 7.

Again, smooth piecewise continuous concentration profiles for all of the solutes were obtained. The first injection, which involved substrate, resulted in a momentary overshoot in the Aceph concentration profile, followed by gradually decreasing concentrations thereafter due to the reaction. The Phel concentration took an initial jump during the first injection of Aceph, followed by repeated jumps due to Phel injections. The dissolved water concentration again showed a similar behavior to that shown in Fig. 5. The reaction rates of Aceph to Phel declined markedly as a function of increasing Phel concentrations, from ca. 4×10^{-5} mol/(min g_{cat}) at ca. 1×10^{-3} M Phel to ca. 2×10^{-5} mol/(min g_{cat}) at ca. 1×10^{-2} M Phel.

3.2.3. Different hydrogen partial pressures and the reaction rates

Experiments 4–6 were performed to address the effects of various hydrogen partial pressures on the reaction rates. At $t = 10$ min, 60 μL of acetophenone was injected into the reaction system through the high-pressure liquid chromatography injection valves at three different hydrogen partial pressures (1.28, 2.49, and 2.98 bar). Concentration profiles of the substrate and product Phel at various hydrogen partial pressures are plotted in Fig. 8.

The reaction rates of Aceph to Phel at different hydrogen partial pressures are plotted in Fig. 9. This figure shows that

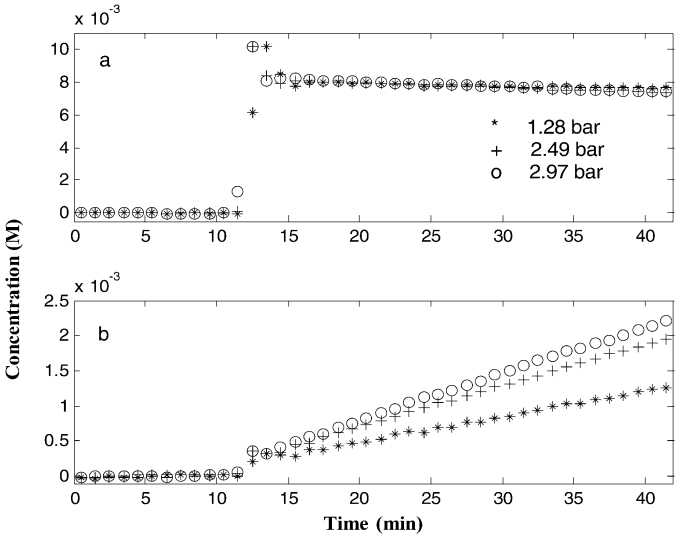

Fig. 8. The concentration profiles of Aceph, Phel at different hydrogen partial pressures. (a) Aceph; (b) Phel.

at similar substrate concentrations, the reaction rates increased with increasing pressure. The reaction rates were shown to be first order with respect to the hydrogen partial pressure (1–3 bar).

3.3. LHHW modeling and kinetic analysis

3.3.1. Assumptions and simplifications

As mentioned in the Introduction, the hydrogenation of acetophenone in the presence of Pt/Al_2O_3 is comparatively more

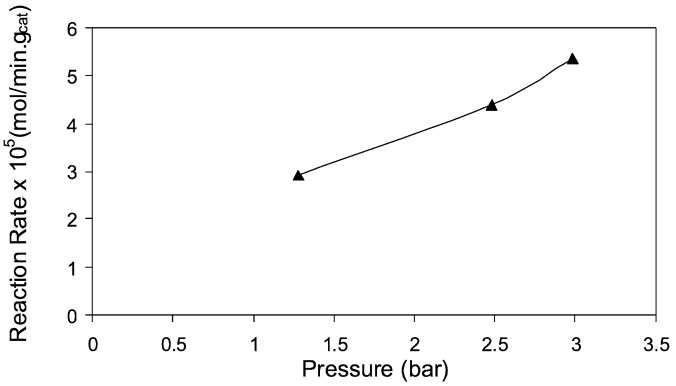

Fig. 9. The reaction rates for the formation of 1-phenylethanol as a function of different hydrogen partial pressures.

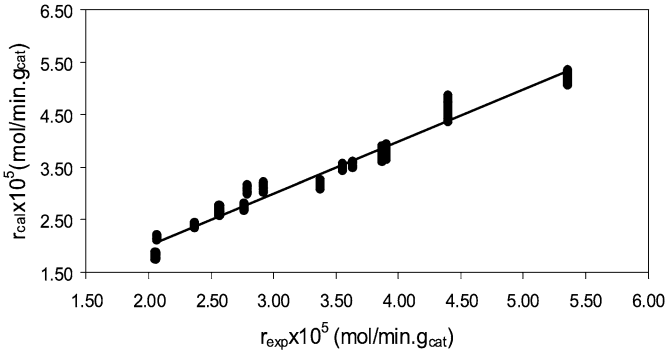

Fig. 10. Comparison of experimental data with the best-fit model for acetophenone hydrogenation to Phel.

complex than simple ketone hydrogenation on metals such as Raney nickel. However, with a few judicious simplifications, modeling of the present system becomes tractable. Most of these assumptions are related to the magnitude of the competing reactions and the magnitude of the associated adsorption equilibrium constants.

Accordingly, the following assumptions for kinetic fitting with the LHHW models can be made:

(i) Methylcyclohexane, the hydrogenated product of h_8-toluene, has a very low concentration throughout the experiments (<0.01% of solution) and it does not adsorb strongly on platinum.
(ii) CMK does not have a high adsorption equilibrium constant (especially compared with Aceph, Phel, and water) and thus does not occupy a significant percentage of active sites on platinum.
(iii) Che has a very low concentration and does not have a high adsorption equilibrium constant (especially compared with Aceph, Phel and water) and thus does not occupy a significant percentage of active sites on platinum.

3.3.2. Model comparison and analysis

With the above judicious simplifications, the adsorption of methylcyclohexane, CMK, and Che can be omitted from the models. The elementary steps considered for the hydrogenation of acetophenone on Pt/Al_2O_3 include competitive adsorption of substrate, product, water and solvent on the same active sites, dissociative or nondissociative adsorption of H_2; and stepwise or pairwise addition of hydrogen to adsorbed substrate. By assuming different rate-limiting steps, 11 different LHHW models were constructed. Details of these models are given in the supplementary material (Part 4). The partial pressure of hydrogen gas, rather than the dissolved hydrogen concentration in the liquid phase, was used in the above rate equations because Henry's law can be applied in this low-pressure range (1–3 bar). In this far-from-equilibrium study, the reverse surface reactions were neglected, and the corresponding rate expressions for the product formation could be reduced.

After omitting a few models that were obviously inconsistent with the experimental rate data, the concentrations of different species under different reaction conditions were used to fit the remaining rate equations. The solvent concentration was assumed to be constant due to the low concentrations of the other species. Nonlinear regression was used to fit the models to the experimental concentration and the rate data for acetophenone hydrogenation to Phel. To determine the best model for describing the reaction rate, the following criteria were used: physical reasonableness of the parameters (i.e., positive values for the estimated adsorption and the rate constants), the residual sum of squares, and parity plots (the actual data plotted against the model values).

The model involving the pairwise addition of dissociated hydrogen to adsorbed substrate as rate-limiting step gave the lowest mean residual sum of squares, that is, the squared difference between the model and the experimental data. The rate expression for this model in given the following:

$$r = \frac{k K_H K_A C_A P_{H_2}}{(1 + \sqrt{K_H P_{H_2}} + K_A C_A + K_P C_P + K_W C_W + K_S C_S)^3}, \quad (1)$$

where k is the reaction rate constant for the rate-limiting step, the K's are equilibrium constants, the C's are concentrations, P_{H_2} is the partial pressure of hydrogen, and the subscripts A, H, P, S, and W refer to Aceph, hydrogen, Phel, solvent, and water, respectively. The complete six sets of experimental reaction rates are compared with the corresponding sets of the fit reaction rates in Fig. 10. The absence of any systematic deviation indicates that the selected best-fitting model accurately describes the formation of Phel from Aceph hydrogenation. The regressed parameters for the best-fitting model are listed in Table 3.

4. Discussion

4.1. Rapid initial hydrogenation of substrate on the fresh and hydrogen-rich catalyst

The initial rate of hydrogenation of Aceph on the fresh and hydrogen-covered catalyst was unusually high. Indeed, there was a significant observable jump in the concentrations of Phel and CMK after the first Aceph perturbation in d_8-toluene at $t = 10$ min. After injection of 20 μL of Aceph (ca. 1.7×10^{-4} mol), and within 10 min, a measurable amount of Phel (ca. 2.2×10^{-5} mol) and CMK (ca. 4.5×10^{-6} mol) were

Table 3
Regression parameters for LHHW model with a pair-wise addition of dissociated hydrogen to the adsorbed substrate as rate-limiting step

k (mol/(min g))	K_H (l/atm)	K_A (l/mol)	K_P (l/mol)	K_W (l/mol)	K_S (l/mol)
$0.005 \pm 4E{-}05$	$0.21 \pm 2E{-}05$	10.24 ± 0.20	11.33 ± 1.73	200.26 ± 5.79	$0.05 \pm 7E{-}04$

formed. During the next 10 min, only an additional ca. 1×10^{-5} mol of Phel and ca. 2×10^{-6} mol of CMK were formed.

Before the first perturbation, the catalyst surface was covered only by adsorbed dissociated hydrogen and adsorbed solvent molecules. Under such a situation, Aceph can rapidly displace the toluene, and rapidly hydrogenate on the hydrogen-rich surface, leading to the almost immediate appearance of the products. The observation of this phenomenon was made possible, to a significant degree, by the very sensitive on-line FTIR measurements.

The number of surface platinum sites on the ca. 0.02 g of catalyst was ca. 7.6×10^{17} or 1.3×10^{-6} mol, and the number of surface sites on the support surface was ca. 2.6×10^{19} or 4.3×10^{-5} mol. The sum of Phel and CMK, formed quickly after the first Aceph perturbation, was ca 1.6×10^{19} or 2.7×10^{-5} mol. Comparison of these numbers seems to indicate that spillover hydrogen was involved in the initial product formation. There is simply not enough dissociated hydrogen on platinum alone before the substrate injection to account for the pulse of the products produced.

4.2. Displacement of reactants on the catalyst support surface

Due to the functional groups present, and in part to the wide range of unsaturation/saturation in the organic reactants used, a wide variation in adsorption equilibrium coefficients on the platinum crystallites is expected. Indeed, this is confirmed by the values listed in Table 3, which were obtained from the regression of the best-fitting LHHW model. The results indicate that the adsorption equilibrium coefficients of the reagents follow the order $K_{water} > K_{aceph} \approx K_{phel} \gg K_{toluene}$ on *platinum*.

The perturbation experiments lead to a number of very interesting short time-scale phenomena, one of which is desorption of species. This is perhaps best exemplified by the first Phel perturbation at the 165th spectrum, which was conducted in d_8-toluene (indicated by the arrows in Fig. 2). The introduction of Phel into the system led to a marked sudden increase in substrate Aceph.

Although this desorption is very interesting, the absorption coefficient ordering of species on the platinum does not seem to be the primary reason for this observation. Approximately, 1.3×10^{18} molecules of Aceph were desorbed by the first Phel perturbation. Because the number of platinum surface sites on the 0.02-g catalyst was only 7.6×10^{17}, the desorption event indicates that there was coverage of adsorbed Aceph on the support before the perturbation and that this coverage decreased on the injection of Phel. Because the surface area of the reaction system was only ca. 49 cm^2, compared with the surface area of 2.66×10^4 cm^2 for the 0.02-g catalyst, the contribution of the experimental apparatus to the complex responses was minimal.

$$2H^* + Aceph^* \overset{k}{\Rightarrow} Phel^* + 2^*$$

Fig. 11. The proposed rate-limiting step for Aceph hydrogenation to Phel at low temperatures and low hydrogen pressures.

4.3. Proposed reaction mechanism

Kinetic studies of the liquid-phase hydrogenation of simple ketones have been studied extensively by several groups. Generally, either the first or second H addition was the rate-determining step depending on the catalyst and the reaction conditions (i.e., temperature, pressure, reaction phase, and solvent) [31–33]. However, pairwise addition has been suggested in some cases. For example, Chang et al. [34] proposed a pairwise addition of dissociated hydrogen to adsorbed ketone on Raney nickel as the rate-limiting step. Hydrogenation of several simple ketones, including acetone, methyl ethyl ketone, methyl *n*-propyl ketone, and diethyl ketone, appears to be consistent with this rate-limiting step.

The best-fitting model in the present contribution is also consistent with a pairwise hydrogen addition mechanism. The elementary steps involved for Aceph hydrogenation to Phel on Pt/Al_2O_3 at 0 °C and low hydrogen partial pressures appear to be competitive adsorption of substrate, water, Phel, and solvent on the same active sites; dissociative adsorption of hydrogen; and pairwise irreversible addition of dissociated hydrogen to adsorbed substrate. The surface reaction is the rate-limiting step as depicted in Fig. 11, where * indicates an adsorbed species.

4.4. Effect of water on reaction rates

As indicated in Section 3.1.2, injection of water into the reaction system resulted in decreased rates of catalytic hydrogenation. Although the reaction performed in d_8-toluene was not 100% anhydrous in the period $t = 0$–265 min, very little water was present and it had very little apparent effect on the hydrogenation kinetics. Only after the deliberate introduction of water at $t = 265$ min (the 232th spectrum) was a significant decrease in hydrogenation kinetics observed.

The marked effect of water on the reaction rates is clearly due to the magnitude of the adsorption equilibrium constant for water, as indicated by Table 3. The adsorption equilibrium constants on platinum have the ordering $K_{water} > K_{aceph} \approx K_{phel} \gg K_{toluene}$. Therefore, water made a statistically significant contribution to the competitive adsorption on the catalyst surface.

These results have important implications for the study of liquid-phase heterogeneous catalysis. They suggest that nontraditional anhydrous experiments serve a very useful purpose and should be implemented whenever possible. The high sensitivity

to trace water exhibited by this reaction also suggests that water variation should be more routinely included in the evaluation of LHHW models.

4.5. Presence of hydrogen bonding

Water is known to hydrogen-bond to many oxygen-containing organic compounds. Such hydrogen bonding can lead to changes in absorptivity of the oxygen-containing moieties, as well as shifts in the corresponding characteristic vibrations. But the spectral data measured in the present experiments did not exhibit any particularly noteworthy changes, at least when the more-or-less anhydrous spectra were compared with those involving the deliberate addition of water. Accordingly, there is little reason to believe that any significant errors or artifacts have arisen in the multivariate analyses, particularly in the concentration profiles.

5. Conclusion

On-line FTIR liquid-phase measurements and multivariate tools were used to successfully analyze the heterogeneous hydrogenation of acetophenone over Pt/Al_2O_3 in d_8-toluene/h_8-toluene. The combination of very precise on-line spectroscopy and the numerical techniques yielded some unexpected phenomenological information. In particular, some of the complex observations seem to be consistent with (i) the presence of spillover hydrogen on the support and its involvement in initial hydrogenation, (ii) adsorption/desorption events involving the reactants on the support, and (iii) the inhibitory effect of water on the catalytic reactions. The methodology also permitted accurate quantitative information on concentrations and reaction rates. The resulting best-fitting LHHW model involved the pairwise addition of dissociated hydrogen to the adsorbed ketone as the rate-limiting step, in which water had a crucial inhibitory effect due to its large adsorption equilibrium constant and hence its ability to displace organic reactants.

Supplementary material

The online version of this article contains additional supplementary material.

Please visit DOI: 10.1016/j.jcat.2006.04.024.

References

[1] J.D. Roberts, M.C. Caserio, Basic Principles of Organic Chemistry, Benjamin, New York, 1965, p. 426.
[2] B. Elvers, S. Hawkins, W. Russell, Ullmann's Encyclopedia of Industrial chemistry, vol. A 15, VCH, New York, 1990, p. 91.
[3] P.S. Kumbhar, M.R. Kharkar, G.D. Yadav, R.A. Rajadhyaksha, J. Chem. Soc., Chem. Commun. (1992) 584.
[4] M.A. Aramendia, V. Borau, J.F. Gómez, C. Jiménez, J.M. Marinas, Appl. Catal. 10 (1984) 347.
[5] M.A. Aramendia, V. Borau, J.F. Gómez, A. Herrera, C. Jiménez, J.M. Marinas, J. Catal. 140 (1993) 335.
[6] P.S. Kumbhar, Appl. Catal. 96 (1993) 241.
[7] A. Alba, M.A. Aramendia, V. Borau, C. Jimenez, J.M. Marinas, Appl. Catal. 17 (1985) 223.
[8] M.A. Aramendia, V. Borau, C. Jiménez, J.M. Marinas, M.E. Sempere, P. Urbano, Appl. Catal. 43 (1988) 41.
[9] S.D. Lin, D.K. Sanders, M.A. Vannice, Appl. Catal. 113 (1994) 59.
[10] D.K. Sanders, S.D. Lin, M.A. Vannice, J. Catal. 147 (1994) 375.
[11] T. Koscielski, J.M. Bonnier, J.P. Damon, J. Masson, Appl. Catal. 49 (1989) 91.
[12] S.D. Lin, D.K. Sanders, M.A. Vannice, J. Catal. 147 (1994) 370.
[13] J. Masson, S. Vidal, P. Cividino, P. Fouilloux, J. Court, Appl. Catal. 99 (1993) 147.
[14] P. Kluson, L. Cerveny, Appl. Catal. 128 (1995) 13.
[15] P. Kluson, L. Cerveny, J. Mol. Catal. A 108 (1996) 107.
[16] C.-S. Chen, H.-W. Chen, W.-H. Cheng, Appl. Catal. 248 (2003) 117.
[17] F. Gao, K.P. Ng, C.Z. Li, K.I. Krummel, A.D. Allian, M. Garland, J. Catal. 237 (2006) 49.
[18] C.Z. Li, E. Widjaja, W. Chew, M. Garland, Angew. Chem. Int. Ed. 41 (20) (2002) 3786.
[19] W. Chew, E. Widjaja, M. Garland, Organometallics 21 (9) (2002) 1982.
[20] E. Widjaja, C.Z. Li, M. Garland, Organometallics 21 (9) (2002) 1991.
[21] C.Z. Li, E. Widjaja, M. Garland, J. Catal. 213 (2) (2003) 126.
[22] C.Z. Li, E. Widjaja, M. Garland, J. Am. Chem. Soc. 125 (18) (2003) 5540.
[23] H.J. Zhang, M. Garland, Y.Z. Zeng, P. Wu, J. Am. Soc. Mass Spectrom. 14 (11) (2003) 1295.
[24] G.E.P. Box, W.G. Hunter, J.S. Hunter, Statistics for Experimenters: An Introduction to Design, Data Analysis, and Model Building, Wiley, New York, 1978, p. 24.
[25] H.U. Blaser, H.P. Jalett, D.M. Monti, J.F. Reber, J.T. Wehrli, Stud. Surf. Sci. Catal. 41 (1988) 153.
[26] M. Garland, H.P. Jalett, H.U. Blaser, Stud. Surf. Sci. Catal. 59 (1991) 177.
[27] D.F. Shriver, M.A. Drezdzon, The Manipulation of Air-Sensitive Compounds, Wiley, New York, 1986.
[28] E. Widjaja, C.Z. Li, M. Garland, J. Catal. 223 (2) (2004) 278.
[29] J.B. Butt, H. Bliss, C.A. Walker, AIChE J. 8 (1962) 42.
[30] D.W.T. Rippin, Ind. Eng. Chem. 6 (1967) 488.
[31] I. Iwamoto, T. Yoshida, T. Aonuma, T. Keii, Nippon Kagaku Zasshi 91 (1970) 1050.
[32] N.O. Lemcoff, J. Catal. 46 (1977) 356.
[33] B. Sen, M.A. Vannice, J. Catal. 113 (1988) 52.
[34] N.-S. Chang, S. Aldrett, M.T. Holtzapple, R.R. Davison, Chem. Eng. Sci. 55 (2000) 5721.